The British Journal of Radiology, 85 (2012), e365–e372

CT and MRI findings of thoracic ganglioneuroma

[1,2]Y B GUAN, [3]W D ZHANG, [2]Q S ZENG, [4]G Q CHEN and [5]J X HE

[1]*Southern Medical University, Guangzhou, China,* [2]*Department of Radiology, The First Affiliated Hospital, Guangzhou Medical College, Guangzhou, China,* [3]*Department of Radiology, State Key Laboratory of Oncology in South China, Cancer Center, Sun Yat-sen University, Guangzhou, China,* [4]*Department of Pathology, The First Affiliated Hospital, Guangzhou Medical College, Guangzhou, China, and* [5]*Guangzhou Institute of Respiratory Diseases, State Key Laboratory of Respiratory Disease, Guangzhou, China*

Objective: Thoracic ganglioneuroma is sporadic and rarely reported. Pre-operative misdiagnosis often occurs in clinical practice. To improve diagnostic accuracy and facilitate differential diagnosis, we summarised the CT and MRI findings of thoracic ganglioneuroma.
Methods: 22 cases of thoracic ganglioneuroma confirmed by surgery and pathology were retrospectively analysed in terms of CT (16 cases) and MRI data (6 cases).
Results: Of 22 lesions, 19 occurred in the posterior mediastinum, 2 in the lateral pleura and 1 in the right chest. The CT value of the plain scans ranged from 20 to 40 HU (mean 29.1 HU) in 16 cases. Punctate calcification was noted in four cases. Patchy fat density shadow was found in one case. Arterial-phase CT found nearly no enhancement (6 cases) or slight enhancement (10 cases) with a CT value of 0–12 HU (mean 5.8 HU). In the delayed phase, enhancement was strengthened progressively, and CT value of 10–20 HU (mean 13.6 HU) was achieved after 120 s. T_1 weighted images showed homogeneous hypointense signals in five cases and hypointense signals mixed with patchy hyperintense signal shadow in one case. T_2 weighted images demonstrated heterogeneous hyperintense signals in all six cases, of which the whorled appearance was noted in one case. Gadolinium-diethylenetriaminepentaacetic acid (Gd-DTPA)-enhanced MRI found mildly heterogeneous enhancement in the arterial phase, and progressive mild enhancement in the delayed phase.
Conclusion: Thoracic ganglioneuroma shows hypodensity in plain CT. On CT and MRI, non-enhancement or slight enhancement in artery phase and progressive mild enhancement in delay phase are characteristic manifestations of ganglioneuroma in the thorax.

Received 22 April 2011
Revised 10 August 2011
Accepted 22 August 2011

DOI: 10.1259/bjr/53395088

Ganglioneuroma is a rare benign tumour of the sympathetic nervous system, usually originating from primitive neural crest cells, and occasionally arising in the adrenal gland medulla. It often occurs in the retroperitoneal space and posterior mediastinum [1–3]. Though abdominal ganglioneuroma is often summarised in the literature [3–7], thoracic ganglioneuroma is sporadic and rarely reported [8–13]. Because there is a lack of knowledge about thoracic ganglioneuroma, pre-operative misdiagnosis often occurs in clinical practice. We here retrospectively summarised CT and MRI findings of 22 cases of thoracic ganglioneuroma to improve the diagnosis accuracy.

Materials and methods

Clinical data

22 cases of thoracic ganglioneuroma confirmed by surgery and pathology were collected from July 2002 to December 2010. The subjects comprised 15 males and 7 females ranging in age from 4 to 57 years, with a median of 21 years. 14 subjects were aged under 20 years and 6 under 10 years. 20 cases were found by chest radiograph, comprising 16 cases without complaint during health examination and 4 cases with cough, influenza and fever. Two cases were found by CT scan: one with cough and shortness of breath during sleep, and one hospitalised because of latent pain of chest and back.

CT scan

16 patients underwent plain and contrast-enhanced CT. Toshiba's Aquilion 16 Multi-Slice CT and Aquilion 4 Multi-Slice CT (Toshiba, Otawara, Japan) were applied, with tube potential of 135 kV, current of 350 mA, field of view (FOV) of 250×250 mm, acquisition slice thickness of 2 mm and reconstruction slice thickness of 7 mm. Contrast-enhanced CT followed plain CT when the patient was asked to stay still. Non-ionic contrast medium iohexol, iodine 300 mg ml^{-1} and flushing 40 ml normal saline were injected from the right antecubital vein using a dual syringe CT injector at a rate of 4.0 ml s^{-1}. Multiphase scan was administered at 30 s, 60 s and 120 s after injection of contrast agent in 12 cases, and at 30 s and 60 s in 4 cases.

Address correspondence to: JianXing He, Guangzhou Institute of Respiratory Diseases, State Key Laboratory of Respiratory Disease, Guangzhou 510120, China. E-mail: jianxing63@163.com
Both YB Guan and WD Zhang contributed equally to the work.

The plain CT scan and 30 s contrast-enhanced CT scan of total lung are used to find lesions in lung and mediastinum, while the aims of 60 s and 120 s contrast-enhanced CT scan are to target tumours. A lead coat was used to protect the sex organs and head in young patients.

MRI examination

Six patients underwent plain and multiphase contrast-enhanced MRI. A Philips Twinspeed (Philips Healthcare, Best, Netherlands) dual gradient system (1.5 T) was applied. Horizontal T_1 and T_2 weighted images, and coronal T_2 weighted images were obtained using spectral selection attenuated inversion recovery (SPAIR). T_1 weighted imaging was performed using turbo spin echo (TSE) sequence with the following parameters: repetition time TR=200–400 ms, echo time TE=4.6–11 ms, matrix 512×512, acquisition time 2–4 times, slice thickness 7 mm and slice distance 2 mm. T_2 weighted imaging was performed using TSE sequence with TR=1300–1500 ms, TE=800–1100 ms, matrix 512×512, acquisition time of 2–4 times, slice thickness of 7 mm and slice distance of 2 mm. Gadolinium-diethylenetriaminepentaacetic acid (Gd-DTPA) was administered with a dose of 0.1 mmol kg^{-1}. Axial, coronal and sagittal multiphase scan was administered. The delayed time was 30, 120 and 240 s after injection of contrast agent.

Two experienced imaging technicians were responsible for analysis of CT and MRI. Findings were analysed regarding the morphology, size, density, signal, calcification, margins and enhancement. Consensus was reached after discussion, if disagreement arose between them.

Results

CT findings

Among 16 lesions, 14 were located in the posterior mediastinum in the paravertebral sulcus (Figure 1a–d) and 2 were in the lateral pleura (Figure 2a, b). The lesions were round or oval with a size of $1.2 \times 2.0 \times 2.0$ cm to $21 \times 15 \times 18$ cm. Plain CT revealed hypodensity with a CT value of 20–40 HU (mean 29.1 HU). Homogeneous density was observed in eight cases and slightly heterogeneous density was observed in the other eight cases. Punctate calcification was noted in four cases (Figures 2a, b, 3a–c). Patchy fat density shadow was found in one case (Figure 2a–c). 12 cases underwent contrast-enhanced and multi-phase scans (Table 1). Non-enhancement (n=6) or mild enhancement (n=6) was noted in 12 cases in the arterial phase with an enhancement difference of 0–12 HU (average: 5.8 HU). Progressive patchy or strip-like enhancement was shown in the delayed phase. The CT value at 120 s was 10–20 HU, with an average of 13.6 HU. The other four cases had mild enhancement in the arterial phase, with enhancement difference less than 20 HU at 60 s. The margins of the lesions at the pulmonary side were clear. Unclear boundaries with adjacent pleura were noticed in eight cases (Figure 3a–c). A pleural effusion was noted in one case. No invasion or damage was noted in adjacent chest wall, ribs and thoracic vertebrae. No enlargement was observed in intervertebral foramens.

MRI findings

Six cases underwent MRI. Five lesions were located in the posterior mediastinum in the paravertebral sulcus, and one occupied the right chest without clear origins (whether from posterior mediastinum or lateral pleura; Figure 4a–d). The lesions were oval or round with clear margins. T_1 weighted images showed homogeneous hypointense signals in five cases and hypointense signals with patchy hyperintense signal shadow (fat tissue) in one case (Figure 5a–c). T_2 weighted images demonstrated heterogeneous hyperintense signals mixed with patchy and linear hypointense signals in all six cases, of which the whorled appearance was noted in one case (Figure 4b). Gd-DTPA-enhanced MRI found mildly heterogeneous patchy or vessel-like enhancement in the arterial phase, and progressive mild enhancement in the delayed phase at 120 and 240 s. Five of them showed macular, patchy or strip-like enhancement. The capsule of the lesion was clearly revealed in all six cases. A pleural effusion was noted in one case (Figure 4d).

Surgery, pathology and immunohistochemistry

22 lesions were resected. Eight lesions showed pleural adhesion, and four of them had very tight pleural adhesion. 12 lesions were closely connected with adjacent sympathetic trunk or intercostal nerves. Macroscopically, the margins of the lesions were clear. They were oval or round, with a complete capsule (Figure 1f, g). The surface of the section was red in 12 cases, grey–white in 6 cases (Figures 1e–g, 5d) and yellow in 4 cases. The lesions were firm in texture in 13 cases, and soft (resembling fish flesh) or gelatinous in 9 cases. No evident bleeding or cystic change was observed. Microscopically, abundant nerve fibres were observed in wavelike or intertwined shape or adipose tissue, with scattered mature ganglion cells (Figures 2c, d, 5e). The nucleus was short and fusiform without mitosis. Partial mucous degeneration was observed with invasion of matrix lymphocytes. Immunohistochemistry was carried out in 14 cases and showed S-100 positive (Figure 2e) and Vim positive (Figure 2f). 10 cases were neuron-specific enolase (NSE) positive (Figure 2g), 8 cases were neuronfilament protein positive and 5 cases were myelin basic protein positive. These markers indicated nerve origins of the lesions.

Misdiagnosed cases

Prior to operation, four cases were misdiagnosed by CT as neurilemmoma, two as cystic teratoma, two as bronchocoele or lymphangioma, two as pleural endothelioma and one as pulmonary blastoma. Four cases were misdiagnosed by MRI as neurilemmoma and one case as embryonic tumour.

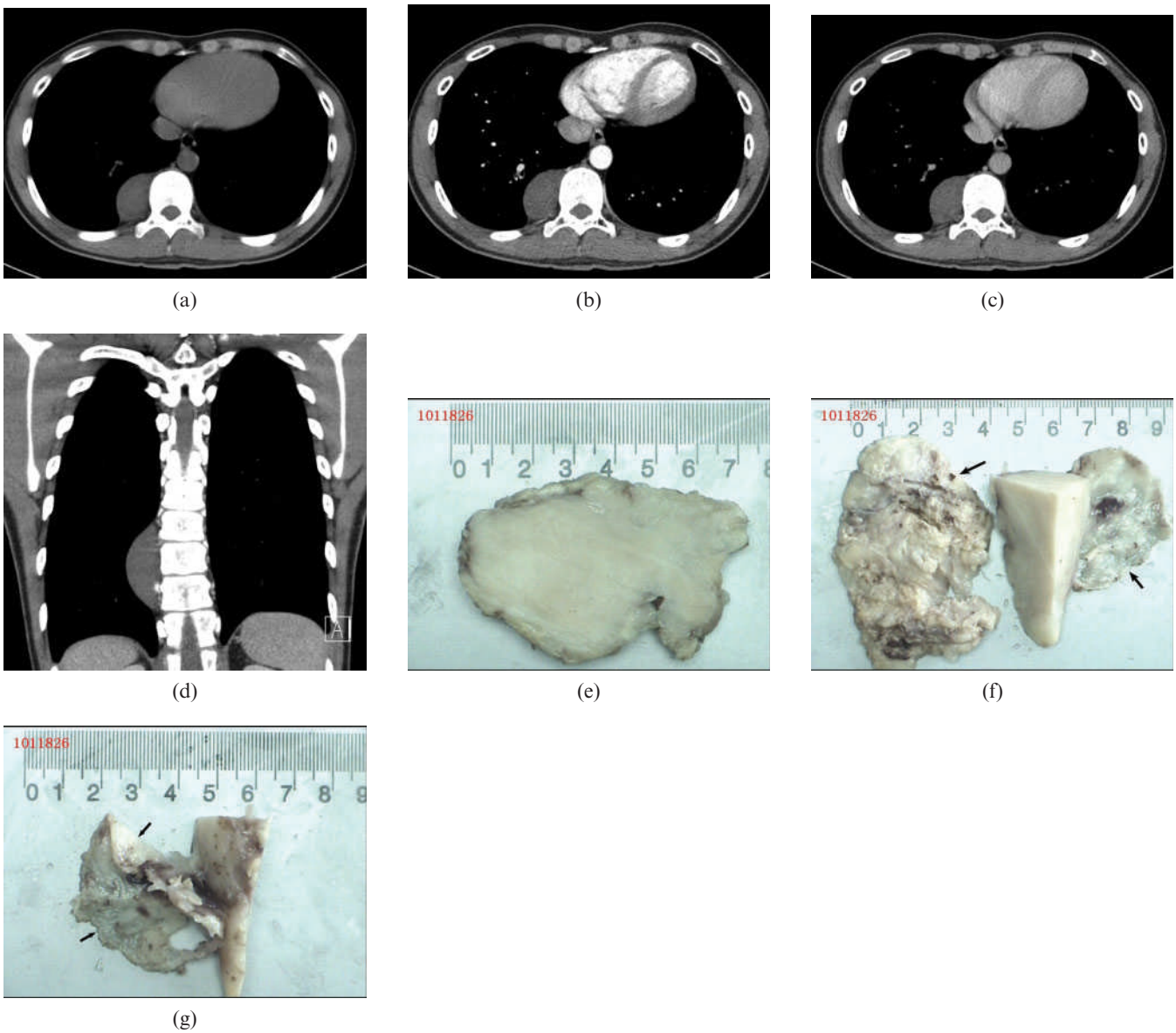

Figure 1. A 22-year-old man with ganglioneuroma in the right posterior mediastinum with a size of 6.7 × 4.5 × 2.5 cm. (a) The plain CT value was about 33 HU. (b) The CT value was about 39 HU in the arterial phase. (c) The CT value was about 46 HU in the delayed phase, with homogeneous density and clear boundaries with adjacent mediastinal pleura. (d) Coronal section showed that the lesion was in the posterior mediastinum. (e–g) Macroscopic pathology showed grey smooth section with complete separate capsule; the tumour is well encapsulated (long arrow in f, g).

Discussion

Ganglioneuroma arises from the autonomic nervous system, most commonly the peripheral sympathetic system. It is often seen in children and adolescents, without distribution difference among males and females [1]. It is generally an asymptomatic mass found on routine chest radiography. It grows slowly, and appears large when it is identified [10]. In the current case series, most (19/22; 86%) were in the posterior mediastinum. 14 subjects were under 20 years of age. The male/female ratio was 2.1:1. They were mostly asymptomatic round or oval tumours with varying sizes, the largest occupying the whole chest with a maximum diameter of 21 cm. Surgical resection is the method of choice to achieve a complete cure [14]. Different surgical styles were applied towards benign and malignant tumours. Additionally, surgical styles might be different when treating ganglioneuroma (solid tumour) and other benign cystic tumours, including large cystic teratoma, bronchocoele and oesophageal cyst and lymphangioma cysticum, which were aspirated before total surgical resection. Therefore, accurate pre-operative diagnosis is essential for treatment.

Ganglioneuroma comprises nerve fibres, Schwann cells, mature ganglion cells and mucous matrix [1]. Diagnosis is made dependent on observation of ganglion cells. When mucous matrix accounts for a large proportion, CT reveals hypodensity, while T_2 weighted imaging shows hyperintense signals. When ganglion cells and nerve fibres increase, CT reveals increased density, while T_2 weighted imaging shows slightly hyperintense signals. Heterogeneous hypointense signals in lesions on T_2 weighted imaging correspond to ganglion cells and nerve

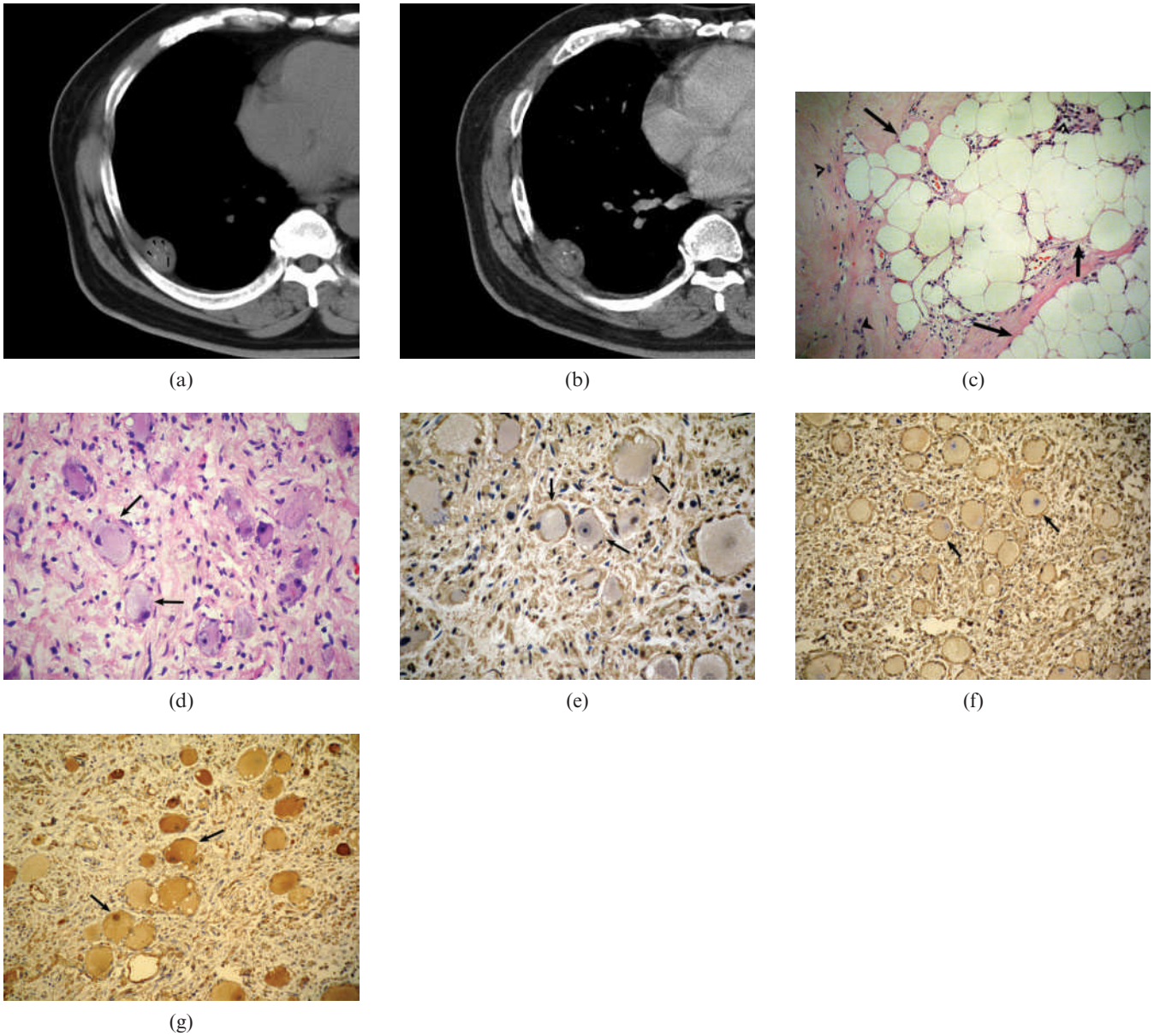

Figure 2. A 53-year-old man with ganglioneuroma. An oval mass was found by plain CT in the right pleura with a size of 3.2 × 2.0 × 2.0 cm. (a) Its solid component showed a CT value of 37 HU. It contained scattered punctate calcification. Strip-like hypodensity was revealed in the lesion with a CT value of −56 HU (fat tissue). (b) The CT value of the solid component was about 52 HU in the delayed phase. (c) Microscopic picture demonstrated abundant fat tissue (long arrow). In addition, Schwann cells (arrowheads) and nerve fibres were observed in wavelike or intertwined shape (original magnification 20 ×). (d) High-power picture showed scattered mature ganglion cells (long arrow), The nucleus was short and fusiform without mitosis (original magnification × 40). (e–g) Immunohistochemistry showed that ganglion cells were S-100 positive (long arrows in e; original magnification × 40). Vim (f) and NSE (g) immunostain confirms the presence of ganglion cells (long arrows; original magnification × 20).

fibres [5]. In the current study, plain CT revealed hypodensity in 16 lesions. Macroscopically homogeneous or heterogeneous cystic density was observed. T_2 weighted imaging images found curved or linear hypointense signals scattered among the hyperintense signals, presenting with a whorled appearance. These hypointense signals represent scattered Schwann cells and collagenous fibres. Lonergan et al [2] consider that the whorled appearance is a typical feature of ganglioneuroma. In this study, however, only one case presented with the whorled appearance; similarly, it is also rarely reported in the literature.

Some researchers regard adipose tissue in the posterior mediastinal lesion as a characteristic feature for diagnosis of ganglioneuroma [9, 11, 13]. Only two cases in our study showed adipose tissue, and they were misdiagnosed pre-operatively due to lack of knowledge. This radiographic feature may be useful in the evaluation of posterior mediastinal masses [9], but needs to be differentiated from teratoma.

It is reported that approximately 10–25% cases of ganglioneuroma are accompanied with calcification [3]. Some researchers believe that the morphology of calcifications can be used to distinguish benign lesions

Table 1. CT and MRI manifestations in 22 patients with intrathoracic ganglioneuroma

			CT findings					MRI findings			
					Enhancement			Plain scan			
Patient number	Sex	Age (years)	Calcification	CT value (HU)	30 s (HU)	60 s (HU)	120 s (HU)	T_1WI	T_2WI	Enhancement (30 s)	Delayed phase
1	F	20	No	30	42		46				
2	M	4	No	20	22		32				
3	M	4	No	32	38		46				
4	M	4	No					Low	Inhomogeneous high	Inhomogeneous slight	Inhomogeneous moderate
5	F	8	No	27	28		40				
6	M	19	No					Low	Inhomogeneous high	Inhomogeneous slight	Inhomogeneous mild
7	F	18	Yes	28	30		38				
8	M	34	No					Low	Inhomogeneous high	Inhomogeneous slight	Inhomogeneous moderate
9	F	14	No	29	33		49				
10	M	8	No					Low	Inhomogeneous high	Inhomogeneous slight	Inhomogeneous moderate
11	F	31	Yes	40	42		50				
12	M	53	Yes	37	44		52				
13	F	57	No	33	41	46					
14	M	21	No	28	28	35					
15	M	15	No					Low	Inhomogeneous high	Inhomogeneous slight	Inhomogeneous mild
16	M	19	Yes	28	36	36					
17	M	3	No	24	33		38				
18	M	46	No	25	35		40				
19	M	11	No	27	35	45					
20	M	14	No					Inhomogeneous low	Inhomogeneous high	Inhomogeneous slight	Inhomogeneous mild
21	F	47	No	25	33		36				
22	M	22	No	33	39		46				

F, female; HU, Hounsfield unit; M, male; T_1WI, T_1 weighted imaging; T_2WI, T_2 weighted imaging.

from malignant lesions [6]. Scattered spotty or grain-like calcification indicates benign lesions, while large patchy or irregular calcification implies malignant tendencies. In this study, 4 (25%) cases presented with scattered macular and punctate calcification, similar to the literature report. As dermoid cyst also often presents with calcification, differential diagnosis should be made with caution.

Because a large amount of mucous matrix exists in ganglioneuroma, cell components are enhanced, while mucous matrix is non-enhanced. Delayed enhancement is mainly owing to blocked perfusion of contrast agent by mucus. The current cases were not apparently enhanced, or only manifested capsule or intratumour linear mild enhancement in the arterial phase. The maximum enhancement value was 12 HU (mean: 5.8 HU). MRI revealed mild enhancement in six cases. Progressive patchy or strip-like enhancement was shown in the delayed phase. CT value at 120 s was 10–20 HU with an average of 13.6 HU. Studies demonstrate that thoracic ganglioneuroma has imaging characteristics similar to abdominal ganglioneuroma [1–6], which may aid accurate diagnosis of ganglioneuroma over the body.

In this study, eight lesions had unclear boundaries with adjacent medistinal pleura and apical pleura, while the margin of the lesions at the pulmonary side was clear. Surgery found pleural adhesion of the lesions with a complete capsule. The capsule was not sensitively revealed in MRI but shown in T_1 weighted imaging. Six lesions revealed circular enhancement by T_1 weighted imaging, possibly due to the complete capsule of tumours.

Thoracic ganglioneuroma needs to be differentiated from other tumours [8, 13, 15, 16]. Cystic teratoma is round with multiple cavities, as well as calcification in the cystic wall. CT may reveal fat density and calcification shadow in the lesion. MRI shows heterogeneous signals: the cystic area has long T_1 and T_2 signals, the fat has high T_1 and T_2 signals, and calcification has low signals. The cystic wall shows linear enhancement while its content is not enhanced in contrast-enhanced MRI. Fat, calcification and fat tissue/fluid level are specific for cystic teratoma. In the current case series, two lesions showed fat density/signals that were progressively mildly enhanced in contrast-enhanced CT. They were thus not diagnosed as cystic teratoma. Bronchocoele and oesophageal cyst are congenital mediastinal cystic lesions with homogeneous density higher than water. Bronchocoele can be present in any area of medistinum, but mostly in the upper or middle section, while oesophageal cyst is mostly in the posterior medistinum. These two diseases are not enhanced in the early phase and delayed phase. Lymphangioma cysticum is rare. It is a congenital malformation of lymph tissues. It contains multiple cavities lined with epithelia. Typical CT characteristics of lymphangioma cysticum include thin walls, and round or oval water-density shadow with multiple cavities. Its CT value ranges from 0 to 20 HU. If

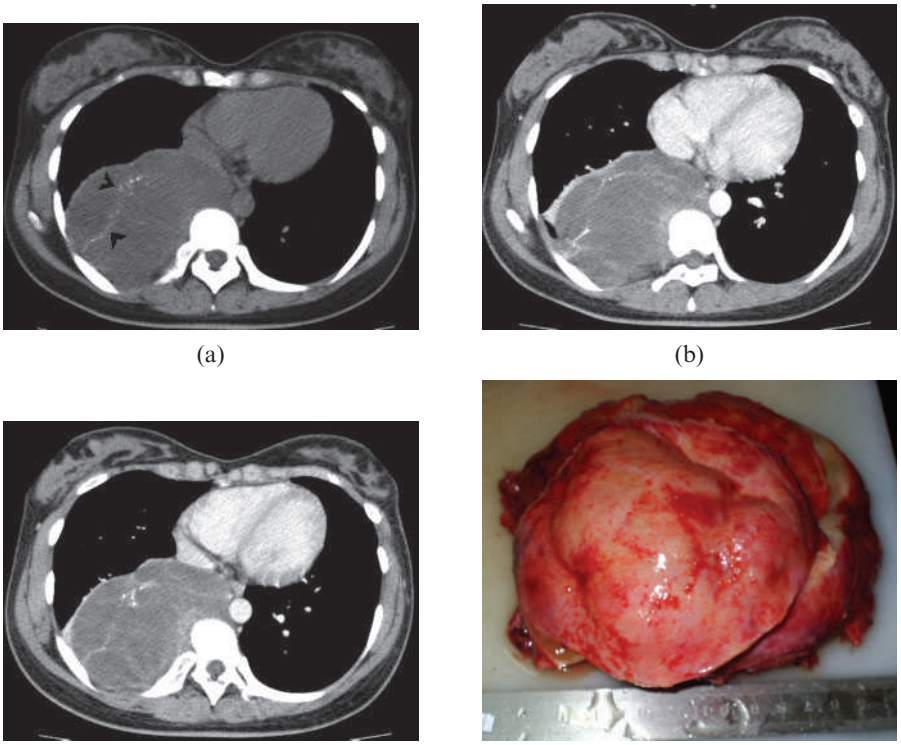

(a) (b) (c) (d)

Figure 3. An 18-year-old girl with a mass in the right posterior mediastinum. (a) Plain CT scan revealed a mass of $6.9 \times 11.5 \times 13$ cm with a CT value of 28 HU and linear and punctate calcification (arrowheads). (b) Patchy enhancement was observed with a CT value of 30 HU in the arterial phase. (c) The CT value was 38 HU in the delayed phase. The boundaries between the lesion and the adjacent mediastinal pleura were not clear. (d) An oval mass with coarse and even red surface, as well as complete capsule, was seen in the photograph of the gross specimen.

it is accompanied by infection or bleeding, the cyst may contain solid components, but calcification is rarely seen. Its surface is mostly smooth. MRI of the cystic area shows long T_1 and T_2 signals. Contrast-enhanced scans reveal mild linear enhancement of the cystic wall and non-enhancement of the cystic fluid. Conversely, ganglioneuroma is progressively enhanced in the delayed phase. MRI signals of mixed Antoni A and Antoni B neurilemmoma are similar to ganglioneuroma. Both are characterised by apparent high signals mixed with moderate signals. However, as neurilemmoma has a propensity to cystic change, its high signals are from

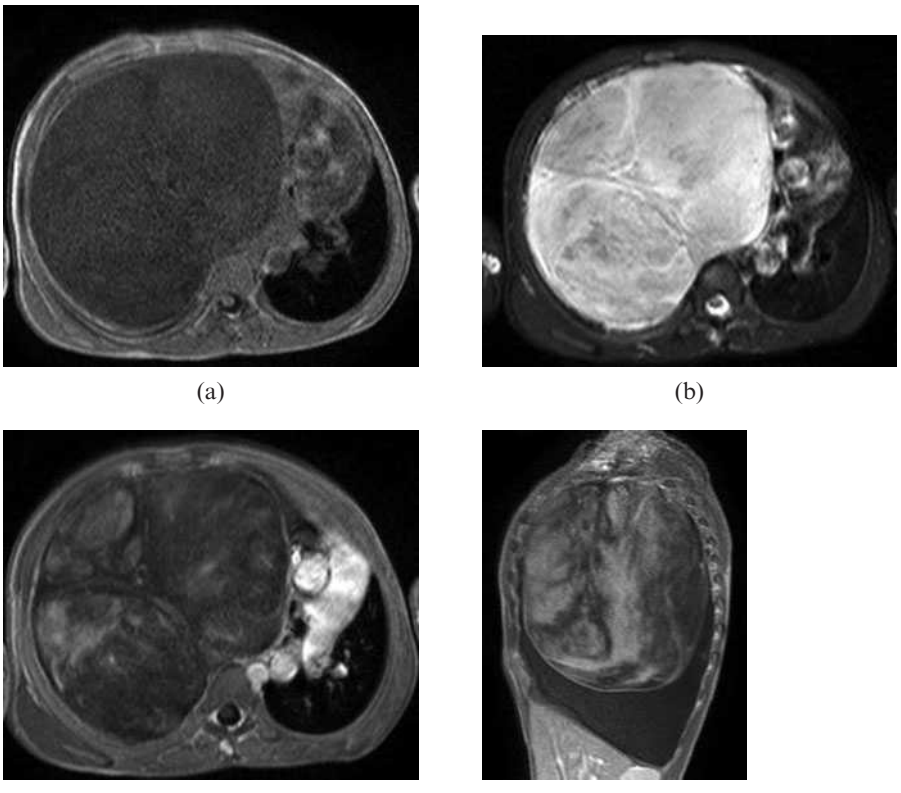

(a) (b) (c) (d)

Figure 4. An 8-year-old boy with a very large oval mass occupying much of the right hemithorax, with an associated pleural effusion. (a) T_1 weighted imaging revealed homogeneous hypointense signals. (b) T_2 weighted imaging revealed heterogeneous hyperintense signals mixed with curve hypointense signals, indicated as a whorled appearance. (c) Axial T_1 weighted image in the arterial phase and (d) sagittal T_1 weighted image in the delayed phase, showing patchy and strip-like enhancement progressed.

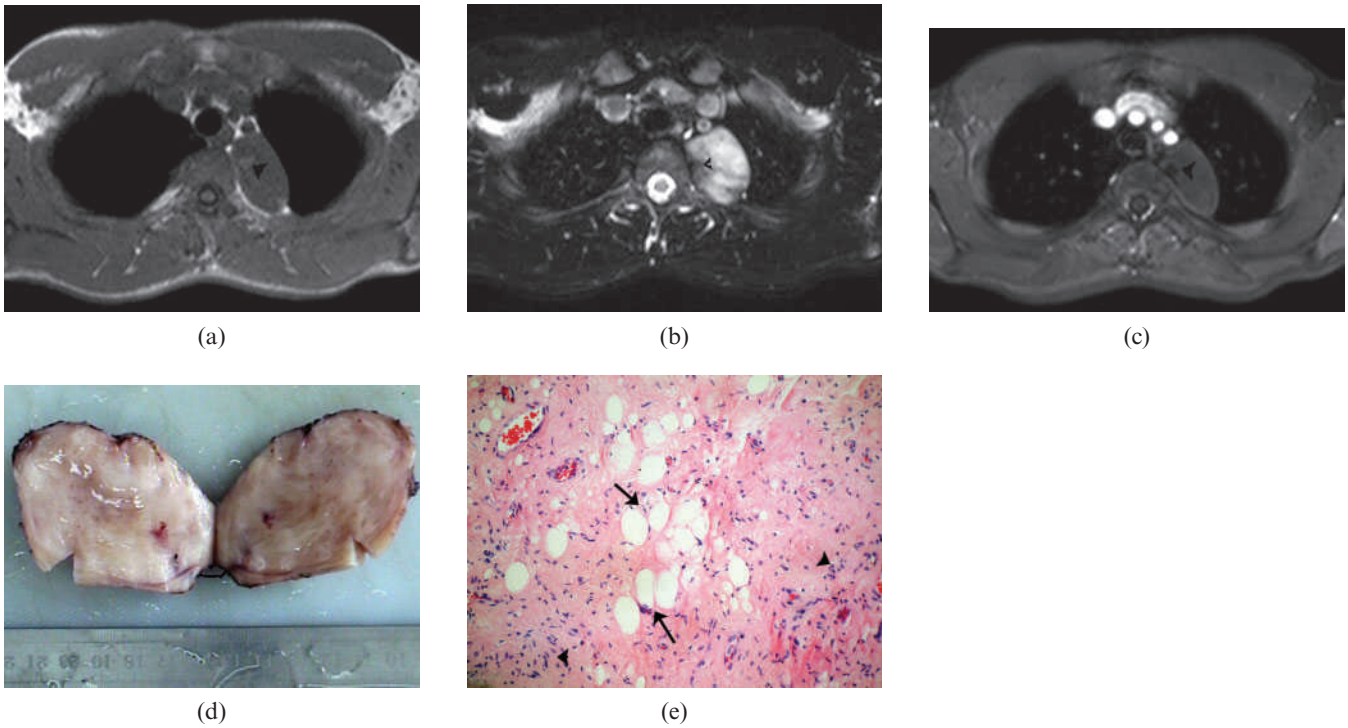

Figure 5. A 14-year old boy with a mass in the left posterior mediastinum. (a) T_1 weighted imaging showed hypointense signals mixed with patchy hyperintense signal (arrowhead). (b) T_2 weighted imaging showed fat suppression signals mixed with high and low signal (arrowhead). (c) Fat suppression was revealed with mild heterogeneous enhancement in T_1 weighted imaging, while hypointense signals (fat tissue, arrowhead) were observed in the hyperintense signal area in T_2 weighted imaging. (d) A grey soft-tissue mass with a size of $7 \times 5 \times 3$ cm was observed, with red intertwined components and a complete capsule. (e) Microscopic picture demonstrated adipose tissue (long arrow), Schwann cells (arrowheads) and nerve fibres (original magnification $20 \times$).

cystic change and necrosis, and the boundaries between high and low signals are clear. For ganglioneuroma, the high and low signals are mingled together. In CT and MRI, neurilemmoma has heterogeneous density/signals, mostly enhanced moderately and even enhanced apparently in the arterial phase, while ganglioneuroma has homogeneous density/signals, enhanced or non-enhanced in the arterial phase and progressively mildly enhanced in the delayed phase. Other sympathetic nervous system tumours should also be differentiated from ganglioneuroma. Ganglion-origin tumours include lowly differentiated neuroblastoma, partially mature ganglioneuroblastoma and completely mature ganglioneuroma. Neuroblastoma and ganglioneuroblastoma are evidently enhanced early and may invade adjacent tissues and blood vessels. They may have osseous metastasis with coarse calcification in the lesions and show early enhancement in imaging.

CT scan of thoracic ganglioneuroma shows hypodensity and non-enhancement or mild enhancement in the early phase. It is often misdiagnosed pre-operatively as cystic teratoma, bronchocoele, neurilemmoma and lymphangioma cysticum. Long T_1 and T_2 signals in MRI may lead to misdiagnosis of neurilemmoma and dermoid cyst. We think that lack of knowledge in imaging technicians and clinicians may lead to misdiagnosis, especially when CT or MRI scanning is not standardised. In the current study, some cases only had arterial-phase or delayed-phase scan, so the enhancement level or process could not be accurately revealed.

Multiphase CT scan can cause high radiation dose for patients and influence the health of patients, especially for young people and children. Therefore, a lead coat is routinely employed to protect these patients in our hospital. Additionally, 60 s and 120 s contrast-enhanced CT scans are to target tumours. Indeed, MRI scan does not use radiation and is the preferred method. However, due to the limited number of cases (six), more studies and cases are needed for drawing the conclusion that MRI method precedes CT method for diagnosis of thoracic ganglioneuroma.

Conclusion

Thoracic ganglioneuroma is a solid tumour at the benign end of the spectrum, occurring predominantly in children and adolescents. Plain CT scan shows homogeneous or heterogeneous hypodensity, accompanied with punctate calcification. Some lesions have fat density, presented as heterogeneous high signals in T_2 weighted images. Some cases show the whorled appearance, presented as non-enhancement or mild enhancement in the arterial phase of CT or MRI and progressive mild enhancement in the delayed phase. Delayed imaging at 120 seconds after contrast enhancement may therefore improve diagnostic accuracy.

References

1. Forsythe A, Volpe J, Muller R. Posterior mediastinal ganglioneuroma. RadioGraphics 2004;24:594–7.

2. Lonergan GJ, Schwab CM, Suarez ES, Carlson CL. Neuroblastoma, ganglioneuroblastoma, and ganglioneuroma: radiologic–pathologic correlation. Radiographics 2002; 22:911–34.
3. Johnson GL, Hruban RH, Marshall FF, Fishman EK. Primary adrenal ganglioneuroma: CT findings in four patients. AJR Am J Roentgenol 1997;169:169–71.
4. Wu YH, Song B, Xu J, Chen WX, Zhao XF, Jia R, et al. Retroperitoneal neoplasms within the perirenal space in infants and children: differentiation of renal and non-renal origin in enhanced CT images. Eur J Radiol 2010;75:279–86.
5. Cai J, Zeng Y, Zheng H, Qin Y, T K, Zhao J. Retroperitoneal ganglioneuroma in children: CT and MRI features with histologic correlation. Eur J Radiol 2010;75:315–20.
6. Ichikawa T, Ohtomo K, Araki T, Fujimoto H, Nemoto K, Nanbu A, et al. Ganglioneuroma: computed tomography and magnetic resonance features. Br J Radiol 1996; 69:114–21.
7. Otal P, Mezghani S, Hassissene S, Maleux G, Colombier D, Rousseau H, et al. Imaging of retroperitoneal ganglioneuroma. Eur Radiol 2001;11:940–5.
8. Sakai F, Sone S, Kiyono K, Maruyama A, Ueda H, Aoki J, et al. Intrathoracic neurogenic tumors: MR–pathologic correlation. AJR Am J Roentgenol 1992;159:279–83.
9. Duffy S, Jhaveri M, Scudierre J, Cochran E, Huckman M. MR imaging of a posterior Mediastinal ganglioneuroma: fat as a useful diagnostic sign. AJNR Am J Neuroradiol 2005;26:2658–62.
10. Maruyama R, Tanaka J, Maehara S, Saeki H, Kinjo M, Higashi H. Intrathoracic ganglioneuroma in an elderly patient over 70 years of age. Gen Thorac Cardiovasc Surg 2007;55:437–9.
11. Hara M, Ohba S, Andoh K, Kitase M, Sasaki S, Nakayama J, et al. A case of ganglioneuroma with fatty replacement: CT and MRI findings. Radiat Med 1999;17:431–4.
12. Ikezoe J, Sone S, Higashihara T, Morimoto S, Arisawa J, Kuriyama K, et al. CT of intrathoracic neurogenic tumours. Eur J Radiol 1986;6:266–9.
13. Ko SM, Keum DY, Kang YN. Posterior mediastinal dumbbell ganglioneuroma with fatty replacement. Br J Radiol 2007;80:e238–40.
14. Fraga JC, Aydogdu B, Aufieri R, Silva GV, Schopf L, Takamatu E, et al. Surgical treatment for pediatric mediastinal neurogenic tumors. Ann Thorac Surg 2010;90:413–8.
15. Duwe BV, Sterman DH, Musani AI. Tumors of the mediastinum. Chest 2005;128:2893–909.
16. Feinstein RS, Gatewood OM, Fishman EK, Goldman SM, Siegelman SS. Computed tomography of adult neuroblastoma. J Comput Assist Tomogr 1984;8:720–6.